Shaping of Intense Ion Beams into Hollow Cylindrical Form

U. Neuner,* R. Bock, M. Roth, and P. Spiller
GSI Darmstadt mbH, Planckstrasse 1, 64291 Darmstadt, Germany

C. Constantin, U. N. Funk, M. Geissel, S. Hakuli, D. H. H. Hoffmann, J. Jacoby, A. Kozyreva, N. A. Tahir, S. Udrea, and D. Varentsov
TU Darmstadt, Institut für Kernphysik, Schlossgartenstrasse 9, 64289 Darmstadt, Germany

A. Tauschwitz
TU Darmstadt, Institut für Angewandte Physik, Schlossgartenstrasse 7, 64289 Darmstadt, Germany
(Received 28 July 2000)

A specifically tailored plasma lens could shape a high-energy, heavy-ion beam into the form of a hollow cylinder without loss of beam intensity. It has been experimentally confirmed that both a positive as well as a negative radial gradient of the current density in the active plasma lens can be the underlying principle. Calculations were performed that yield the ideal current density distribution for both cases. A numerical simulation of an experiment with an intense ion beam highlights that the shaping of the beam increases the achievable compression in a lead sample.

PACS numbers: 41.85.Ct, 52.40.Mj

A current carrying plasma in the beam line of a high-energy accelerator offers possibilities in ion optics that are beyond the scope of conventional elements. In the latter the currents that produce the magnetic fields are flowing in solids where ions get scattered or even absorbed. Severe restrictions are therefore imposed on the use of conductors in the volume occupied by the beam. A low-density, high-conductivity plasma on the contrary allows current to freely flow in the volume occupied by the beam. This gives additional freedom in the choice of the magnetic field configuration of high-energy ion optical elements.

The shaping of intense ion beams into hollow cylindrical form constitutes a new application of this basic principle. These beams are of essential importance in the production of dense strongly coupled plasmas. Examples from experimental astrophysics and inertial confinement fusion research are given in the end of this Letter.

Hollow cylinder shaped ion beams can, with conventional ion optical elements, only be achieved by overlaying multiple beams or by blocking out the central part of a single beam. Multiple intense ion beams are not yet available, and blocking is inappropriate due to the reduction of the beam intensity. We therefore developed a method to produce a hollow cylinder shaped beam without loss of particles out of a single intense ion beam. An image of the light output of a scintillator showing the ringlike transverse beam profile is depicted in Fig. 1.

The desired beam shaping was achieved with an active plasma lens in a specifically designed operation mode. It deviates from the normal operation where the current in the plasma is axially directed and has a constant density over the ion beam radius. Its magnetic field is azimuthally directed and radially linearly increasing. This field focuses a parallel beam onto a spot [1–6] or, vice versa, a divergent beam from a production target into a parallel beam [7–10]. It is therefore applicable to high-energy beams, in contrast to the electrostatic plasma lens [11,12] for low-energy beams. When working in this standard way the plasma lens focuses a heavy ion beam of 6 T m magnetic rigidity (ion momentum divided by ion charge) to produce the minimum possible beam spot on the target [13–16]. This in turn leads to the highest possible specific deposition energies that are necessary for experiments addressing high-energy density in matter [17]. The beam profile in the focal plane is then Gaussian, imaging the transverse emittance distribution of the beam.

In addition to this standard operation mode a specifically tailored plasma lens can furthermore achieve an almost ideal ring shaped intensity distribution of the ion beam in the focal plane. The minimum width of the ring is limited only by the transverse emittance of the beam. The current is again axially directed, but the current density has a radial gradient. This allows for the two focusing schemes plotted in Figs. 2 and 3. A parallel, zero emittance beam

FIG. 1. 10 mm radius ringlike light output from a scintillator situated perpendicular to the axis 0.3 m behind the plasma lens.

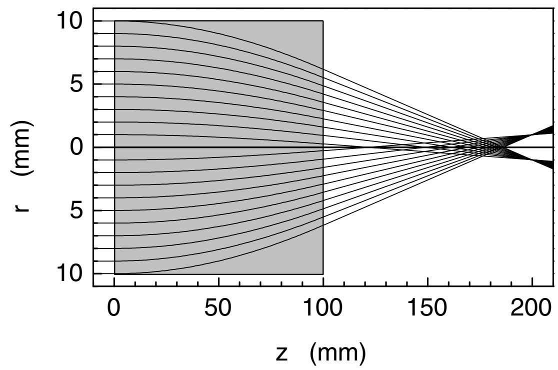

FIG. 2. Schematic of focusing a 10 mm radius parallel ion beam into a 1 mm radius ring with a 100 mm long plasma lens with a negative radial gradient of the current density and a 100 mm long drift length.

of 10 mm radius, represented by 21 ion trajectories, is incident from the left. In the plasma lens, indicated by a rectangle for radii $r \leq 10$ mm and distances along the axis $0 \leq z \leq 100$ mm, the ion trajectories are bent towards the axis according to the Lorentz force in the magnetic field. Following the plasma lens is a drift section, where the ion trajectories are straight lines. At $z = 200$ mm all trajectories converge into a ring in the focal plane.

Figure 4 shows the corresponding current densities in the plasma lens for a 6 T m beam. For the focusing scheme shown in Fig. 2, with the ion trajectories crossing the axis between the plasma lens and the focal plane, the current density exhibits a negative radial gradient (pinch mode). For the focusing scheme of Fig. 3 the current density exhibits a positive radial gradient (skin mode). The current density was calculated by discretization along the radius followed by one-dimensional nonlinear optimizations. For every current distribution the magnetic field was calculated using Ampere's law. The current feed at the entrance ($z = 0$) and exit ($z = 100$ mm) of the plasma lens was assumed to be purely in the radial direction. The angular momentum of the ions was taken to be zero. The ion trajectories were calculated in paraxial approximation. The part of the beam that is incident at radii smaller than 1 mm is in both cases not focused onto the ring in the focal plane. The radial dependence of the current density for radii smaller than 1 mm can be chosen arbitrarily, only its normalization is given by the deflection of ions entering the lens at 1 mm radius. For the negative gradient case we chose a current density distribution for radii smaller than 1 mm that leads to a smooth decrease of the current density with radius. For the positive gradient case we chose a constant value.

Along the axis a range of roughly 2 cm around the focal plane exists (190 mm $\lesssim z \lesssim$ 210 mm) where the ring profile is sustained and the beam is hollow cylinder shaped. As illustrated in Fig. 2 the radius of this hollow cylinder increases with distance from the plasma lens for the case of a negative radial gradient of the current density. For the positive radial gradient case the radius of the hollow cylinder decreases with distance from the plasma lens, as shown in Fig. 3.

Measurements were performed with a 3 T m carbon beam of 80 ns pulse length. In the plasma lens the current carrying plasma is produced in a pulsed gas discharge with a strongly damped oscillating current. The duration of the first current half wave is 9 μs, and the maximum current is 240 kA. The diameter of the discharge volume is 20 mm, and its length is 90 mm. The working gas was argon at 3.6 mbar. Hollow cylinder shaped ion beams were achieved during phases of the z-pinch discharge, where the current density is not radially constant. These phases do exist before and after the phase of constant current density, which is located in time between 3.2 and 3.7 μs after the initiation of the discharge.

An image intensified CCD camera recorded the light output of a thin plate of a cerium-doped quartz scintillator (M382, HERAEUS Quarzschmelze GmbH, Germany) positioned perpendicular to the axis in the drift section behind the plasma lens. These images were azimuthally averaged to yield the transverse beam profiles.

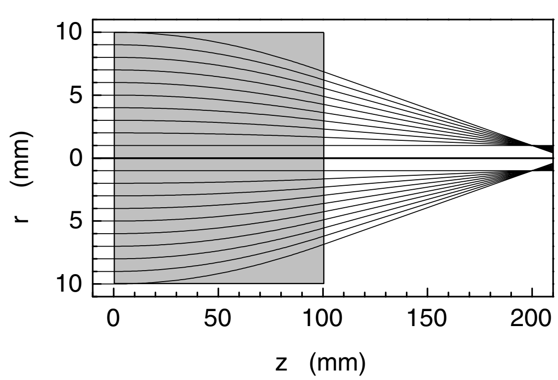

FIG. 3. Schematic of focusing a 10 mm radius parallel ion beam into a 1 mm radius ring with a 100 mm long plasma lens with a positive radial gradient of the current density and a 100 mm long drift length.

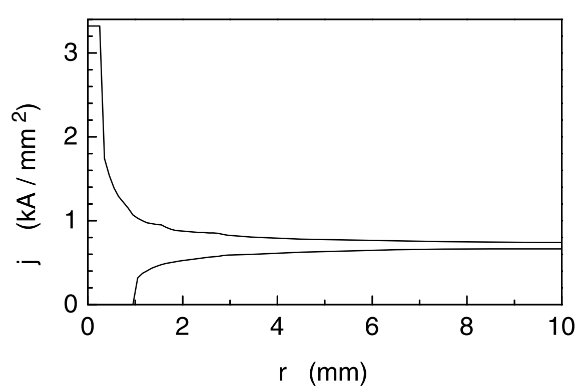

FIG. 4. Calculated current density in the plasma lens as a function of radius that leads to focusing into a ring, as shown in Fig. 2 (upper curve) and Fig. 3 (lower curve).

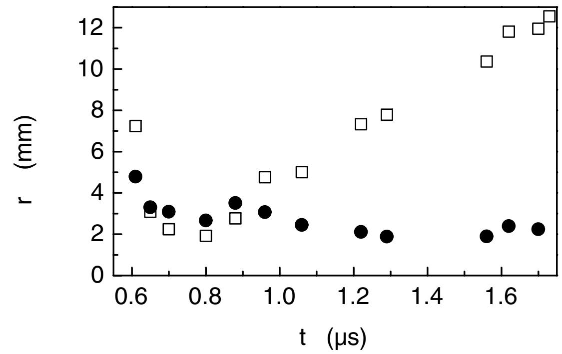

FIG. 5. Measured radius (open squares) and width (HWHM) (filled circles) of the hollow cylinder shaped beam in a plane 0.3 m behind the plasma lens as a function of time after the initiation of the plasma lens discharge.

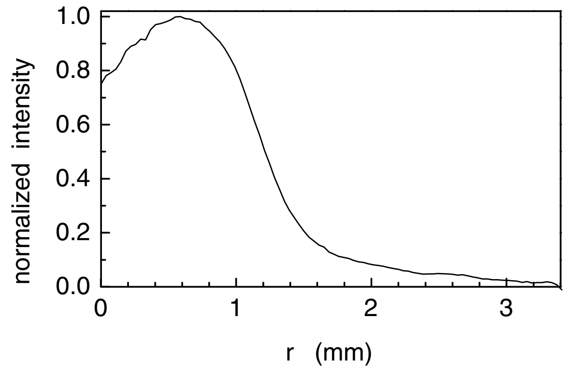

FIG. 7. Radial profile of the beam intensity distribution in the detection plane 0.1 m behind the plasma lens for the case of the minimum radius of 0.58 mm.

The duration of stable focusing must match the pulse length of future intense high-energy, heavy-ion beams. Therefore Fig. 5 shows the measured radius (maximum of the profile) and width (half width at half maximum, HWHM) of the ringlike beam intensity distribution in a plane 0.3 m behind the plasma lens exit as a function of time after initiation of the plasma lens discharge. The radius stays constant to within $\pm 10\%$ for 110 ns, long enough for the future intense beam pulses of typically 50 ns duration. The radial velocity of the hollow cylinder shape, i.e., the time derivative of its radius, overall varies between -0.1 mm/ns and 0.025 mm/ns. The highest aspect ratio achieved between radius and width of the ring was 25, measured at a time later than shown in Fig. 5, but here a substantial part of the beam was incident in the area around the axis and the intensity in the ring was about to drop to zero.

The highest contrast achieved between the maximum ion beam intensity and the intensity on the axis was 10. The corresponding radial profile is shown in Fig. 6. (This measurement corresponds to the data point at 1.56 μs in Fig. 5 and also to the image shown in Fig. 1.)

In another series of measurements the distance between the exit of the plasma lens and the detection plane was reduced to 0.1 m. Here the minimum radius of 0.58 mm was achieved, the corresponding profile is shown in Fig. 7. This measurement also corresponds to the minimum width (HWHM) of the ring shaped beam profile of 0.6 mm, taken from the right-hand wing of the profile. This is a factor of 2 higher than the emittance limit, and therefore shows that the actual current density in the plasma lens does not exactly resemble one of those depicted in Fig. 4 and that there is still a potential for further optimization.

The hollow structure prevailed over 10 mm in the axial direction. The radius increased with distance from the plasma lens, from 0.58 to 1.2 mm, indicating a negative radial gradient of the current density, as mentioned before. Whereas this measurement was performed during a late phase of the plasma lens discharge, namely, 6.22 μs after its initiation, with the current carrying plasma pinched around the axis, another measurement with a 5 T m argon beam was carried out during an early phase, i.e., 1.27 μs after the discharge initiation. It resulted in a radius that decreases with distance from the plasma lens, from 1.7 to 1.2 mm, measured at 52 and 82 mm distances, respectively. This is, as mentioned before, indicative of a positive radial gradient of the current density, typical for the skin-effect-dominated early phase of a z-pinch discharge.

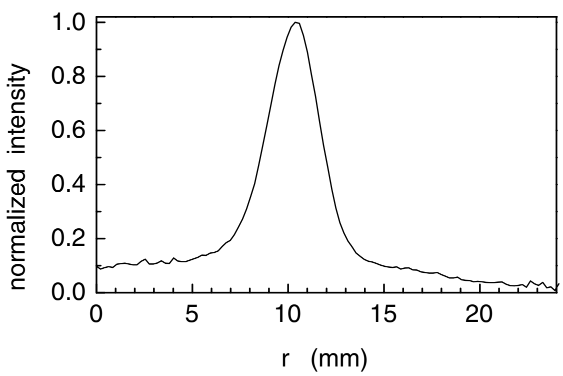

FIG. 6. Radial profile of the beam intensity distribution in the detection plane 0.3 m behind the plasma lens for the case of the optimum contrast of 10.

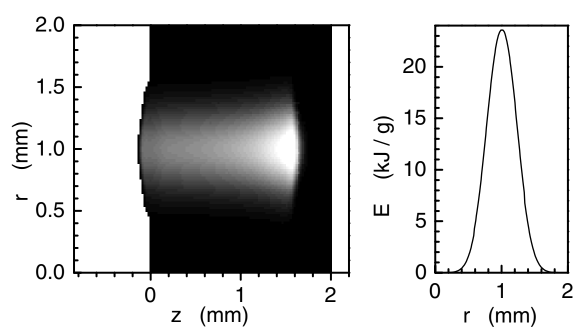

FIG. 8. Numerical simulation of a heavy-ion-driven cylindrical implosion in lead. Left: deposited specific energy at the end of the ion pulse. Right: radial profile at $z = 1.05$ mm.

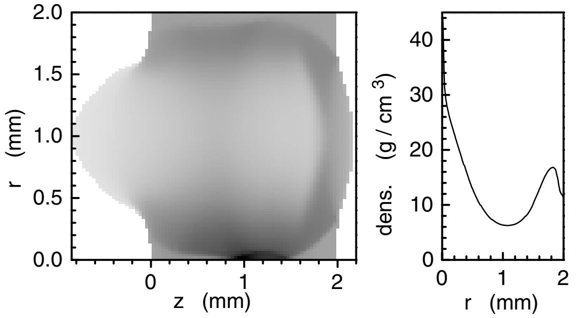

FIG. 9. Numerical simulation of a heavy-ion-driven cylindrical implosion in lead. Left: density at the time of maximum compression on the axis. Right: radial profile at $z = 1.05$ mm.

Hollow cylinder shaped intense beams of high energetic heavy ions are efficient drivers for implosion targets to create matter in a highly compressed state. Future experiments have been numerically simulated both for spherical and for cylindrical compression. Spherical compression can be achieved in close-coupled distributed radiator, heavy-ion targets, where the beam energy is converted into x-rays which then drive the implosion of an embedded spherical capsule to achieve D-T fusion by inertial confinement [18,19]. Cylindrical compression can be achieved by irradiating a cylindrical converter and employing the thermal expansion of the heated hollow cylindrical volume to achieve compression on the axis.

Two-dimensional numerical simulations of such an experiment were performed for a beam of 2×10^{11} uranium ions at 200 MeV/u kinetic energy, delivered in a parabolic pulse of 50 ns foot-to-foot time, incident on a solid lead target [20]. An intense beam of these parameters is scheduled to be available at GSI's accelerators in the near future. The deposited energy that was taken as an input parameter in this simulation is shown in Fig. 8. With the results that were already achieved in the shaping of intense beams into the form of a hollow cylinder, the radial profile of 1 mm radius and 0.6 mm width (FWHM) seems feasible. The resulting compression is shown in Fig. 9. Its maximum value is 4 times the solid state density. In comparison to former calculations utilizing simple beams with radial Gaussian profiles that were axially centered [21], the utilization of a hollow beam increased the compression by a factor of 2.

As for further improvements, a hollow beam with a radius that is decreasing in time has been proven to be possible (cf. Fig. 5). It could follow the implosion, thereby making it more efficient. Substituting the lead in the central part of the target by solid hydrogen, the production of metallic hydrogen, a key constituent of giant planets, has been predicted [22,23].

We would like to thank A. Shutov for help with the numerical simulation code. This work was supported in part by BMBF.

*Electronic address: u.neuner@gsi.de

[1] E. Boggasch *et al.,* Phys. Rev. Lett. **66**, 1705 (1991).
[2] E. Boggasch *et al.,* Appl. Phys. Lett. **60**, 2475 (1992).
[3] M. de Magistris *et al.,* Nuovo Cimento Soc. Ital. Fiz. **106A**, 1643 (1993).
[4] A. Tauschwitz *et al.,* Nuovo Cimento Soc. Ital. Fiz. **106A**, 1733 (1993).
[5] A. Tauschwitz *et al.,* Laser Part. Beams **13**, 221 (1995).
[6] M. de Magistris *et al.,* Fusion Eng. Des. **32-33**, 377 (1996).
[7] W. K. H. Panofsky and W. R. Baker, Rev. Sci. Instrum. **21**, 445 (1950).
[8] E. B. Forsyth, L. M. Lederman, and J. Sunderland, IEEE Trans. Nucl. Sci. **12**, 872 (1965).
[9] R. Kowalewicz *et al.,* in *Proceedings of the 1991 IEEE Particle Accelerator Conference,* edited by L. Lizima and J. Chew (IEEE, Piscataway, NJ, 1991), pp. 2631.
[10] R. Kowalewicz *et al.,* in *Proceedings of the Third European Particle Accelerator Conference, Berlin 1992,* edited by H. Henke, H. Homeyer, and Ch. Petit-Jean-Genaz (Editions Frontieres, Gif-sur-Yvette, France, 1992), pp. 1539.
[11] D. Gabor, Nature (London) **160**, 89 (1947).
[12] M. Reiser, in *Proceedings of the 1989 IEEE Particle Accelerator Conference,* edited by F. Bennett, and J. Kopta (IEEE, Piscataway, NJ, 1989), pp. 1744, and references therein.
[13] B. Heimrich *et al.,* Nucl. Instrum. Methods Phys. Res., Sect. A **294**, 602 (1990).
[14] M. Stetter *et al.,* Nuovo Cimento Soc. Ital. Fiz. **106A**, 1725 (1993).
[15] M. Stetter *et al.,* Fusion Eng. Des. **32–33**, 503 (1996).
[16] U. Neuner *et al.,* in *Inertial Fusion Sciences and Applications 99,* edited by Ch. Labaune, W. J. Hogan, and K. A. Tanaka (Elsevier, Paris, 2000), p. 559.
[17] D. H. H. Hoffmann *et al.,* Nucl. Instrum. Methods Phys. Res., Sect. B **161–163**, 9 (2000), and references therein.
[18] D. A. Callahan-Miller and M. Tabak, Nucl. Fusion **39**, 1547 (1999).
[19] D. A. Callahan-Miller and M. Tabak, Phys. Plasmas **7**, 2083 (2000).
[20] N. A. Tahir *et al.,* Phys. Rev. E **62**, 1224 (2000).
[21] N. A. Tahir *et al.,* Phys. Rev. E **61**, 1975 (2000).
[22] N. A. Tahir *et al.,* J. Phys. IV (France) **10**, Pr5–327 (2000).
[23] N. A. Tahir *et al.,* Phys. Rev. E (to be published).